*Manuscript
Click here to download Manuscript: Manuscript TO SUBMIT.doc
Click here to view linked References

Sorcin silencing inhibits epithelial-to-mesenchymal transition and suppresses breast cancer metastasis *in vivo*

Yunhui Hu[1,2,3,†], Shuangjing Li[1,4,†], Ming Yang[1], Cihui Yan[1], Dongmei Fan[1], Yuan Zhou[1], Yanjun Zhang[1], Ernesto Yagüe[2,††] and Dongsheng Xiong[1,††]

[1] State Key Laboratory of Experimental Hematology, Department of Pharmacy, Institute of Hematology & Hospital of Blood Diseases, Chinese Academy of Medical Sciences & Peking Union Medical College. Tianjin 300020, China
[2] Division of Cancer, Imperial College London, Hammersmith Hospital Campus, Du Cane Road, London W12 0NN, UK
[3] Department of Breast Cancer, China Tianjin Breast Cancer Prevention, Treatment and Research Center, Tianjin Medical University Cancer Institute and Hospital, Tianjin 300020, China.
[4] Liaocheng People's Hospital，Liaocheng, Shandong Province 252000, China

* To whom correspondence should be addressed. Tel: +44 (0)20 7594 2802; Email: ernesto.yague@imperial.ac.uk
Correspondence may also be addressed to Donseng Xiong, Tel: *+86-22-23909404*; Email: dsxiong@ihcams.ac.cn

[†] These authors contributed equally to this work.
[††] Senior corresponding authors contributed equally

Running Title: Sorcin regulates EMT and breast cancer stem cells

Keywords: sorcin, E-cadherin, EMT, breast cancer stem cells

Word count (excluding Title Page, Abstract, References and Figure legends): 3492

Total number of figures and tables: 5 + 1 Supplementary Table and 2 Supplementary Figures

Abstract

Sorcin, a 22-kDa calcium-binding protein, renders cancer cells resistant to chemotherapeutic agents, thus playing an important role in multidrug resistance. As there is a clear association between drug resistance and an aggressive phenotype, we asked whether sorcin affects also the motility, invasion and stem cell characteristics of cancer cells. We have used both RNA interference (transient and stable expression of hairpins) and a lentiviral expression vector to experimentally modulate sorcin expression in a variety of cells. We demonstrate that sorcin depletion in MDA-MB-231 breast cancer cells reduces the pool of $CD44^{+}/CD24^{-}$ and $ALDH1^{high}$ cancer stem cells as well as mammosphere-forming capacity. We also observe that sorcin regulates epithelial-mesenchymal transition and cancer stem cells partly through E-cadherin and vascular endothelial growth factor expression. This leads to the acquisition of an epithelial-like phenotype, attenuating epithelial-mesenchymal transition and suppression of metastases in nude mice. The sorcin-depleted phenotype can also be reproduced in lung adenocarcinoma A549 cells and lung fibrosarcoma HT1080 cells. In addition, over-expression of sorcin in MCF7 cells, which have low endogenous sorcin expression levels, increases their migration and invasion *in vitro.* This offers the rationale for the development of therapeutic strategies down-regulating sorcin expression for the treatment of cancer.

Introduction

Metastasis and chemoresistance play important roles in tumor recurrence and poor clinical outcome of cancer patients. A small subset of cancer cells, with self-renewal and differentiation features, the cancer stem cells (CSC), are thought to be responsible for resistance to chemotherapy and cancer cell metastasis [1]. Differentiated mammary epithelial cells that have undergone epithelial-to-mesenchymal transition (EMT, a key developmental program activated during cancer invasion and metastasis) have been reported to generate $CD44^{high}CD24^{low}$ stem cell-like cells [2]. In addition, metastatic cells with CSC characteristics are found in a variety of cancers [3,4]. More recently, it has become evident that EMT not only leads to increased metastasis and a CSC phenotype, but directly correlates with drug resistance [5]. In breast cancer, chemoresistance to 5-fluorouracil induces EMT via elevating expression of Snail [6]. Conversely, over-expression of EMT-related transcriptional factors increase multidrug resistance via up-regulation of ABC transporters, while attenuating EMT-inducing transcription factors sensitize breast cancer cells [7]. Such intimate association between EMT and chemoresistance has also been found in a variety of malignancies [8,9]. These lines of evidence may provide us with novel therapeutic strategies to overcome tumor metastasis and recurrence via targeting the EMT, CSC and drug resistance junction.

Sorcin is a 22-kDa calcium-binding protein expressed in many tissues [10] where it regulates Ca^{2+} homeostasis and has been found to be up-regulated in gastric cancer [11]. Sorcin is an histological marker for malignant glioma [12] and forms part of the molecular signature of $CD34^{+}$ haematopoietic stem and progenitor cells of patients with chronic myelogenous leukaemia in chronic phase [13]. In addition, sorcin predicts poor outcome in acute myeloid leukemia [14]. Although the functional role of sorcin in cancer cells remains elusive, it is likely that its antiapoptotic function [15] leads to drug

resistance in a variety of malignant cells [16-17].

Here, we report the role of sorcin in breast cancer metastasis via its effect on EMT and breast CSCs. Using stable silencing (shRNA), we demonstrate that depletion of sorcin attenuates CSCs, increases E-cadherin expression and decreases VEGF expression. This affects both the proportion of CSCs as defined by the $CD44^{+}/CD24^{-}$ and $ALDH1^{high}$ phenotype and their invasive properties in nude mice. These findings offer us the rationale to explore compounds or strategies to experimentally down-regulate sorcin expression in cancer.

Materials and Methods

Cell culture

The breast cancer cell lines MDA-MB-231 and MCF-7, the lung cancer adenocarcinoma cell line A549, the lung fibrosarcoma cell line HT1080 were obtained from The American Type Culture Collection through the Cell Resource Centre of the Chinese Academy of Medical Sciences / Peking Union Medical College, Tianjin, China, and were authenticated by short tandem repeat profiling. Cells were cultured in DMEM (Invitrogen Life Technologies) with 10% fetal calf serum and 2 mM L-glutamine (GIBCO). Cultures were maintained at 37°C in an air-5% CO_2 incubator at constant humidity.

RNA interference

For stable knockdown of sorcin (shSorcin) and for control (shNC), annealed hairpins (Supplementary Table S1) were cloned into pSilencer™ 2.1-U6 hygro and transfected into MDA-MB-231 cells using lipofectamin 2000 (Invitrogen) following the manufacture's standard protocol. Stable transfectants were selected using 800 μg/ml hygromycin (Sigma) and maintained with 50 μg/ml hygromycin. For transient transfections, 21-nucleotide siRNA duplex targeting human sorcin (Supplementary Table S1) and scrambled sequences (control siRNA) were designed using tools available at http://www.ambiom.com and synthesized by Genepharma. The siRNA duplexes were transfected into cells using lipofectamine 2000 according to the recommended protocol by the manufacturer.

Construction of lentivirus expression vectors and cell transfection

An approximately 700-bp DNA fragment corresponding to the full-length of sorcin coding sequence was generated by PCR from pcDNA3.1/sorcin [18] using the primers Sorcin-NheI and Sorcin-NotI

(Supplementary Table S1) and cloned into the lentivirus expression vector pCDH1 (System Biosciences, SBI, USA). Lentiviral transfections were performed into HEK293T cells essentially as described [19] using 20 µg lentiviral plasmid, 2 µg pVSVG, 8 µg pPAX2 (Addgene, Cambridge, Massachusetts, USA) and 60 µl Lipofectamine 2000 (Invitrogen). Viral supernatants were collected 48 hours after transfections, filtered through 0.45 µm pore size filter (Millipore) and supplemented with 8 µg/mL Polybrene (Sigma-Aldrich) prior to infecting MCF-7 cells. Puromycin (1µg/ml; Sigma-Aldrich) was added to the culture medium 96 hours after infection.

Antibodies and Reagents

Antibodies used were C20 for sorcin (Santa Cruz Biotechnology), 14C10 for GAPDH, 24E10 for E-cadherin, D80D3 for ZEB1 (Cell Signaling Technology). Adriamycin was purchased form Pharmacia & UpjohnS.p.A. (Milan, Italy). Etoposide and methylthiazolyldiphenyl-tetrazolium bromide (MTT) were purchased from Sigma (St. Louis, MO).

RNA isolation and real-time reverse transcription-PCR

Total RNA was isolated using Trizol (Invitrogen) following the manufacturer's protocols. The cDNA was generated by using OligdT primers and SuperScriptIII reverse transcriptase (Invitrogen) using 1 µg total RNA. Real-time PCR was perfomed using an ABI SDS7000 (Applied Biosystems, Foster City, CA), in combination with SYBR Green I (Takara). Specific primers for each gene (Supplementary Table S1) were selected using Primer Express (Applied Biosystems). The efficiencies of amplification of each primer pair were in the range 95.3%-99.2%. PCR amplifications included a standard curve for each amplified gene in order to extrapolate transcript amounts from the Ct values. Relative transcript

expression was normalized to that of *GAPDH* mRNA [20].

Protein extraction and western blotting

A modified RIPA buffer (50 mM Tris–HCl, 150 mM NaCl, 0.25% SDS, 1% Triton X-100, 0.25% sodiumdeoxycholate, 1 mM EDTA, 1 mM EGTA, 1 mM dithiothreitol) with protease inhibitor cocktail (Sigma) was used for protein isolation. Protein concentrations were determined using the BCA Protein Assay Kit (Pierce, Rockford, IL, USA). Cell lysates containing 50 μg of total protein were resolved on 12% polyacrylamide gels and transferred to nitrocellulose membranes (Millipore, Billerica, MA, USA), and blocked with 5% blotting grade milk (Bio-Rad, Hercules, CA, USA) in PBST (0.1% Tween 20 in PBS). Then membranes were incubated with primary antibodies at 4°C overnight (dilution 1:100 for sorcin detection, dilution 1:1000 for GAPDH, E-cadherin and ZEB-1 detection), followed by HRP-conjugated secondary antibodies (Cell Signaling Technology) at 1:2000 dilution for 2 hours at room temperature. Signals were visualized using SuperSignal West Pico Chemiluminescent Substrate (PIERCE, Rockford, IL, USA) according to the manufacturer's instructions.

IC_{50}

A MTT assay [21] was used to determine the drug concentrations producing 50% cell growth inhibition (IC_{50}). Cells were seeded and cultured overnight in 96-well plates at a density of 5000 cells/well, followed by incubation with drugs in triplicate.

In vitro growth curves

To determine growth rates, 1×10^4 cells were plated in each well of a 12-well plate (Corning). From the

next day, cells were trypsinized and counted with a haematocytometer every day until day 7.

Wound healing assay

Cells were grown to confluence in a 6-well plate (Corning). After standard wounds were inflicted with a needle tip, images of wounded monolayers were obtained at 0 and 24 h.

Motility and invasion assays

For transwell assays, 1×10^5 cells were plated in the top chamber with the non-coated (motility assay) or Matrigel-coated (invasion assay) transwell inserts containing 8 μm filters (BD Falcon). In both assays, cells were plated in DMEM medium without serum, and DMEM medium supplemented with 20% serum was used as a chemo attractant in the lower chamber. The cells were incubated for 24 h and cells that did not migrate or invade through the pores were removed by a cotton swab. Cells on the lower surface of the membrane were stained with the Diff-Quick Staining Set (Dade Behring) and counted.

Enzyme-linked immunosorbent assay (ELISA)

Cells (3×10^5) were plated in a 6-well plate with DMEM medium supplemented with 10% serum and incubated for 24 h. Medium was replaced with 2 ml serum-free DMEM for another 24 h and then collected for ELISA. Blood was taken from tumor-bearing mice and immediately place into EDTA-treated tubes (BD Biosciences). Plasma was obtained by removing blood cells through centrifugation at 1800 *g* for 15 min. VEGF levels in both the cell culture medium and plasma of mice were measured by a commercial VEGF ELISA kit (R&D Systems) according to the manufacturer's instructions.

Flow cytometry

For cell apoptosis analysis, cells were labelled using an annexin V-FITC and propidium iodide double-staining apoptosis detection kit (Becton Dickinson, Mountain View, CA) according to the manufacturer's instructions. Stem cell markers, FITC-conjugated CD44 and PE-conjugate CD24 (BD Biosciences) were used as described [21]. An Aldefluor assay kit (StemCell Technologies) was used for the determination of aldehyde dehydrogenase activity by flow cytometry as described [22].

Soft agar colony formation assay

Cells were disassociated, suspended in DMEM containing 0.3% agar, and plated onto a bottom layer containing 0.6% agar. The cells were plated at a density of 2 x 10^5 cells/well of 6-well plate, and the colonies were counted and stained with 0.1% crystal violet 21 days later.

Mammosphere culture

Cells (1×10^3) were plated in each well of an ultralow attachment plate (Corning) with 3 ml serum-free mammary epithelial growth medium (MEGM, BioWhittaker), supplemented with B27 (Invitrogen), 20 ng/mL EGF and 20 ng/ mL bFGF (BD Biosciences). Colony formation was assessed 10 days later.

In vivo pulmonary metastatic assay

All animal studies were performed at the Chinese Academy of Medical Sciences & Peking Union Medical College in accordance with guidelines under IACUC and approved by the State Key Laboratory of Experimental Hematology Ethical Committee. Nude mice (5-6 weeks of age; PUMC) were used in

the study and received 400 rad of γ-radiation using a dual 137Cs source 1 day before tumor cell injection. Tumor cells (5×10^6) in 100 μl PBS were injected into the mammary fat pad. Tumor sizes were measured every four days in two dimensions using a caliper, and the tumor volume was calculated with the following formula: tumor volume (mm^3) =0.5 x ab^2 (a and b being the longest and shortest diameters of the tumor, respectively). Approximately 30 days after transplantation, the mammary tumors were removed and weighed. The tumors, lungs, livers and spleens were fixed in 10% buffered formalin and then embedded in paraffin, sectioned and stained with haematoxylin and eosin. The lung metastatic nodules were checked under the microscope.

Statistical analysis

A t-test was used when comparing samples. Statistical significance was considered when $P<0.05$.

Results

Experimental down-regulation of sorcin increases drug sensitivity

We initially found that invasive MDA-MB-231 cells expressed higher levels of sorcin than non-invasive MCF-7 cells (Fig. 1a). To investigate the role of sorcin in malignant tumor metastasis, we generated MDA-MB-231 cells in which sorcin was knocked-down by stable expression of a short hairpin. Two randomly selected clones, MDA-E3 and MDA-D4 (with sorcin down-regulation of approximately 50% at the RNA level and 70% at protein level), were isolated (Fig. 1b). A randomly selected clone, MDA-NC, was picked up from the pool of the transfection with the scrambled sequence and was used as control. The change in sorcin expression was not associated with cell proliferation as both types of cell showed identical growth rates (Fig. 1c). As sorcin is closely associated with multidrug-resistance, we asked whether down-regulation of sorcin could sensitize MDA-MB-231 cells to chemotherapeutic agents. As expected, the adriamycin IC_{50} values decreased by 60-70% (63.7% in MDA-E3 cells and 71.1% in MDA-D4 cells when compared to MDA-NC control cells). Equally, sorcin-depleted cells were more sensitive to etoposide (IC_{50} reduction of approximately 88%; Fig 1d; Supplementary Fig. S1). This change in drug sensitivity following sorcin down-regulation was further confirmed by analyzing apoptosis after etoposide treatement (Fig. 1e). Thus, the experimental down-regulation of sorcin leads to an increase in drug sensitivity.

Sorcin silencing inhibits EMT in MDA-MB-231 cells

As sorcin knock-down led to a change in the morphology of MDA-MB-231 cells (from mesenchymal-like to epithelial-like, Fig. 2a), we asked whether other traits of mesenchymal cells could be regulated by sorcin expression. For this, we initially tested the motility of cells using wound healing assays and found that sorcin-depleted cells were less motile than the corresponding control cells (Fig. 2b). This was

further confirmed quantitatively by using transwell assays (with or without Matrigel) in transient tranfections (Supplementary Fig. S2a) and isolated clones (Fig. 2a-d). These changes in cell morphology, motility and invasion suggest that sorcin silencing compromises EMT progression in MDA-MB-231 cells.

To further investigate how aberrant expression of sorcin leads to phenotypic changes in MDA-MB-231 cells, we monitored some EMT markers. Expression of the most significant epithelial marker, E-cadherin, increased remarkably in MDA-E3 cells and MDA-D4 cells (Fig. 2e,g). Moreover, down-regulation of expression of ZEB-1, a key transcriptional repressor of E-cadherin, accompanied sorcin down-regulation (Fig. 2f,g), indicating another potential regulator linked between sorcin and E-cadherin.

Angiogenesis is an important process for the generation of metastases [2] and VEGF (vascular endothelial growth factor) is a potent mediator of angiogenesis. We found that VEGF-A was markedly reduced at both mRNA and protein levels in sorcin-depleted cells (Fig. 2h). Thus, sorcin silencing leads to the inhibition of EMT in breast cancer cells.

Suppression of sorcin reduces the stem cell sub-population of MDA-MB-231 cells

As sorcin knockdown led to an inhibition of EMT and EMT can generate cells with characteristics of stem cells [1], we asked whether these changes affected also the stemness of MDA-MB-231 cells. We analyzed, first, the expression CD44 and CD24, two cell-surface markers whose expression in the $CD44^{high}/CD24^{low}$ configuration is associated with human breast cancer stem cells [21]. The percentage of $CD44^{high}/CD24^{low}$ cells was reduced in sorcin knock-down cells (Fig. 3a). We then analyzed aldehyde dehydrogenase (ALDH) activity, another important marker of cancer stem cells [23] and found that it

was remarkably diminished in sorcin-depleted cells (Fig. 3b; Supplementary Fig. S2b).

To further assess whether silencing of sorcin influences the stemness and tumorigenicity of tumor cells, we tested both anchorage independence in soft agar, as only stem-cell like cells are able to survive and form clones in non-adherent conditions, as well as mammosphere formation [24]. We observed that sorcin-depleted cells produced less than half the number of mammospheres (Fig. 3c; Supplementary Fig. S2c) and clones in soft agar (Fig. 3d), when compared to control cells.

Thus, experimental down-regulation of sorcin in MDA-MB-231 cells reduces their CSC characteristics and tumor formation.

Silencing of sorcin inhibits MDA-MB-231 cells metastasis *in vivo*

As silencing of sorcin inhibited EMT and reduced the stemness of MDA-MB-231 cells *in vitro*, we asked whether the effects of sorcin depletion on tumor growth and metastasis would be maintained *in vivo*. For this, control (MDA-NC), and sorcin-depleted (MDA-E3 and MDA-D4) cells were injected into the mammary fat pad of nude mice, and tumor size and weight monitored for up to 30 days. As expected, control cells gave raise to tumors which kept growing and finished with sizes of approximately 1500 mm^3 and 1.4 g of weight. However, mice injected with sorcin-depleted cells had much smaller tumors (~250 mm^3 and 0.2 g; Fig. 4a,b). Thirty three days after injection, the tumor and organs were removed for further analysis. Visible lung metastases could be found in all four mice injected with control cells, whereas no metastasis was found in either the MDA-E3 or MDA-D4 group (Fig. 4c). We confirmed that tumors generated from sorcin-depleted cells had a lower expression of sorcin, but higher expression of E-cadherin, than the tumors generated from control cells (Fig. 4d). In addition, the former also showed lower *VEGF* mRNA levels than the latter. This was further confirmed when the VEGF levels in plasma

were determined (Fig. 4e).

Thus, sorcin silencing in MDA-MB-231 cells inhibits tumor growth and metastasis spread *in vivo.*

Effects of sorcin depletion/overexpression on other tumor cells

To further verify the relationship of sorcin with migration and invasion we used breast cancer MCF-7, lung adenocarcinoma A549 and lung fibrosarcoma HT1080 cells. For this, we stably over-expressed sorcin in MCF-7 and transiently knocked-down sorcin by RNA interference in A549 and HT1080 cells. Sorcin mRNA levels increased over 5-fold in MCF-7 and decreased by approximately 60% in A549 and HT1080 cells (Fig. 5a). We then analyzed the motility and invasive properties of these cells in transwells without or with Matrigel, respectively. Down-regulation of sorcin led to a decrease in both the motility and invasion of HT1080 and A549 cells when compared to those transfected with scrambled siRNA (Fig. 5b), whereas overexpression of sorcin improved the migratory and invasive abilities of MCF-7 cells (Fig. 5c). This confirms that the results shown in previous sections are not exclusive to MDA-MB-231 cells, and thus sorcin depletion reverse the invasive phenotype of cancer cells.

Discussion

The findings presented here describe an unexpected convergence of three phenomena of fundamental importance in cancer biology *via* the calcium-binding protein sorcin. On one side, EMT is a key developmental program often activated during cancer invasion and metastasis [16]. On the other, sorcin has been documented as a chemoresistant protein in a variety of cancers [25]. In addition, a small set of tumor-initiating cells (often referred as CSCs) has been suggested to be not only responsible for resistance to chemotherapy, but also for cancer metastasis and tumor recurrence, always accompanied with EMT activation [26-28]. EMT generates cellular traits associated with high-grade malignancy leading to metastatic dissemination; in addition, CSCs induced from EMT are also able to generate drug resistance and poor outcome of cancer patients [5,29]. The close relationship of these processes is evident as chemo-insensitive CSCs selected after chemotherapy treatment can execute the initial steps of the invasion-metastasis cascade that lead in turn to seed the large colonies of cancer cells that form macroscopic metastases [30]. Consequently, understanding of mechanisms underlying the development and association of EMT with chemoresistance is of the outmost significance for improving current therapeutic strategies.

Sorcin, a calcium-binding protein that modulates excitation-contraction coupling in the heart, contributes to calcium homeostasis in the heart sarcoplasmic reticulum and is often associated with drug resistance [31]. We have confirmed that its down-regulation increases adriamycin and etoposide sensitivity in MDA-MB-231 cells. Although the mechanism of drug resistance by sorcin has been poorly studied, it has recently been suggested that it enhances the accumulation of $Ca2^{+}$ in the endoplasmic reticulum (ER) of colorectal cancer cells, thus preventing ER stress [32]. In leukaemia cells, over-expression of sorcin leads to apoptosis evasion by increasing Bcl-2 and attenuating Bax

expression [33]. Sorcin is involved in the regulation of $Ca2^+$ homeostasis in cardiomyocytes [32], but the regulation of $Ca2^+$-mediated signaling pathways by sorcin in cancer is poorly studied. Besides triggering an accumulation of $Ca2^+$ in the ER of colorectal cancer cells, sorcin leads to reduced cytosolic $Ca2^+$ levels in K562 cells [34]. As increased cytosolic $Ca2^+$ levels can lead to apoptosis and decreased content of $Ca2^+$ in the ER is associated with resistance to apoptosis [11], it is tempting to speculate that in breast cancer cells, sorcin silencing may lead to apoptosis by modulating intracellular $Ca2^+$ levels.

Consistent with a positive correlation between sorcin and lymph node metastasis in gastric cancer [35], our results provide evidence that the experimental down-regulation of sorcin in cell systems reverts EMT by elevating E-cadherin expression, a hallmark of epithelial cells, leading to a inhibition of invasion. ZEB-1, a transcriptional factor which negatively regulates E-cadherin expression [36] was also down-regulated in sorcin-depleted cells. Others have reported markers associated also with both chemoresistance and EMT. For instance, the E-cadherin repressor SNAI1 not only enhances the effect of EMT, but also increases chemoresistance in colorectal cancer [37], and in epithelial ovarian cancer, the blockade of endothelin A receptor-driven EMT overcomes chemoresistance and inhibits tumor progression, improving patient outcome [38,39]. In breast cancer cells undergoing EMT, a remodeling of $Ca2^+$ influx pathways, including elevated store-operated $Ca2^+$ entry have been demonstrated [40]. Moreover, a variety of calcium-binding proteins contribute to carcinoma metastasis, including the S100 protein family and SPARC [41-44]. Indeed, S100 proteins are up-regulated in the primary tumors of many cancers and their over-expression is often associated with poor patient prognosis due to their ability to induce cell migration and metastasis [45].

Our results also provide a link between sorcin and CSCs. Although sorcin depletion in

MDA-MB-231 cells does not affect proliferation *in vitro*, it leads to a decrease in the $CD44^{+}/CD24^{-}$ and $ALDH1^{high}$ populations and consequent formation of mammospheres and colonies in soft agar. Others have also described a variety of mechanisms of CSC generation following chemoresistance in breast cancer [46-48]. Whether sorcin regulates EMT and CSCs directly or, more likely, indirectly remains to be determined.

How sorcin regulates VEGF is even more intriguing. Our data shows that down-regulation of sorcin leads to a decrease in VEGF expression both in cell systems and in the tumors of nude mice. Angiogenesis is a hallmark of cancer [22,49] and VEGF mediates a wide range of changes within the tumor vasculature, including cell proliferation, migration, invasion and survival in many solid cancers [50,51]. Importantly, VEGF and intracellular $Ca2^{+}$ levels are frequently associated [52], although the molecular mechanisms remain obscure. It may also be plausible that VEGF signaling represents a "salvage pathway" occurring during the development of chemoresistance.

Discovery of novel molecular targets to reduce the CSC population and inhibit cancer metastasis is of paramount significance. As sorcin depletion reduces breast cancer cells growth and metastasis, impedes angiogenesis *in vivo*, reduces the CSC population and sensitizes cancer cells to chemotherapeutics, this offers the rationale for the development of anti-sorcin therapies in breast cancer.

Acknowledgments

YH acknowledges support from the China Scholarship Council to visit Imperial College London. We thank S. Raguz (Medical Research Council, UK) for her advice on lentiviral expression.

This work was supported by grants from Natural Science Foundation of China (Grant numbers 30873091, 30971291 and 81170512); Natural Science Foundation of Tianjin (Grant number. 05YFGZGX02800); and National Science and Technology Major Project (Grant number 2012ZX09102301-015).

Conflict of Interest

The authors declare no conflict of interest.

The experiments described in the manuscript comply with the current laws of the countries in which they were performed

References

1. Al-Hajj M, Wicha MS, Benito-Hernandez A, Morrison SJ, Clarke MF (2003) Prospective identification of tumorigenic breast cancer cells. Proc Natl Acad Sci U S A 100 (7):3983-3988. doi:10.1073/pnas.0530291100
0530291100 [pii]
2. Mani SA, Guo W, Liao MJ, Eaton EN, Ayyanan A, Zhou AY, Brooks M, Reinhard F, Zhang CC, Shipitsin M, Campbell LL, Polyak K, Brisken C, Yang J, Weinberg RA (2008) The epithelial-mesenchymal transition generates cells with properties of stem cells. Cell 133 (4):704-715. doi:10.1016/j.cell.2008.03.027
S0092-8674(08)00444-3 [pii]
3. Hermann PC, Huber SL, Herrler T, Aicher A, Ellwart JW, Guba M, Bruns CJ, Heeschen C (2007) Distinct populations of cancer stem cells determine tumor growth and metastatic activity in human pancreatic cancer. Cell Stem Cell 1 (3):313-323. doi:10.1016/j.stem.2007.06.002
S1934-5909(07)00066-5 [pii]
4. Giannoni E, Bianchini F, Masieri L, Serni S, Torre E, Calorini L, Chiarugi P (2010) Reciprocal activation of prostate cancer cells and cancer-associated fibroblasts stimulates epithelial-mesenchymal transition and cancer stemness. Cancer Res 70 (17):6945-6956. doi:10.1158/0008-5472.CAN-10-0785
0008-5472.CAN-10-0785 [pii]
5. Dean M, Fojo T, Bates S (2005) Tumour stem cells and drug resistance. Nat Rev Cancer 5 (4):275-284. doi:nrc1590 [pii]
10.1038/nrc1590
6. Zhang W, Feng M, Zheng G, Chen Y, Wang X, Pen B, Yin J, Yu Y, He Z (2012) Chemoresistance to 5-fluorouracil induces epithelial-mesenchymal transition via up-regulation of Snail in MCF7 human breast cancer cells. Biochem Biophys Res Commun 417 (2):679-685. doi:10.1016/j.bbrc.2011.11.142
S0006-291X(11)02170-X [pii]
7. Saxena M, Stephens MA, Pathak H, Rangarajan A (2011) Transcription factors that mediate epithelial-mesenchymal transition lead to multidrug resistance by upregulating ABC transporters. Cell Death Dis 2:e179. doi:10.1038/cddis.2011.61
cddis201161 [pii]
8. Haslehurst AM, Koti M, Dharsee M, Nuin P, Evans K, Geraci J, Childs T, Chen J, Li J, Weberpals J, Davey S, Squire J, Park PC, Feilotter H (2012) EMT transcription factors snail and slug directly contribute to cisplatin resistance in ovarian cancer. BMC Cancer 12:91. doi:10.1186/1471-2407-12-91
1471-2407-12-91 [pii]
9. Zhu K, Chen L, Han X, Wang J, Wang J (2012) Short hairpin RNA targeting Twist1 suppresses cell proliferation and improves chemosensitivity to cisplatin in HeLa human cervical cancer cells. Oncol Rep 27 (4):1027-1034
10. Meyers MB, Pickel VM, Sheu SS, Sharma VK, Scotto KW, Fishman GI (1995) Association of sorcin with the cardiac ryanodine receptor. J Biol Chem 270 (44):26411-26418
11. Deng L, Su T, Leng A, Zhang X, Xu M, Yan L, Gu H, Zhang G (2010) Upregulation of soluble resistance-related calcium-binding protein (sorcin) in gastric cancer. Med Oncol 27 (4):1102-1108. doi:10.1007/s12032-009-9342-5
12. Yokota T, Kouno J, Adachi K, Takahashi H, Teramoto A, Matsumoto K, Sugisaki Y, Onda M, Tsunoda T (2006) Identification of histological markers for malignant glioma by genome-wide expression analysis: dynein, alpha-PIX and sorcin. Acta Neuropathol 111 (1):29-38.

doi:10.1007/s00401-005-1085-6
13. Diaz-Blanco E, Bruns I, Neumann F, Fischer JC, Graef T, Rosskopf M, Brors B, Pechtel S, Bork S, Koch A, Baer A, Rohr UP, Kobbe G, von Haeseler A, Gattermann N, Haas R, Kronenwett R (2007) Molecular signature of CD34(+) hematopoietic stem and progenitor cells of patients with CML in chronic phase. Leukemia 21 (3):494-504. doi:2404549 [pii]
10.1038/sj.leu.2404549
14. Tan Y, Li G, Zhao C, Wang J, Zhao H, Xue Y, Han M, Yang C (2003) Expression of sorcin predicts poor outcome in acute myeloid leukemia. Leuk Res 27 (2):125-131. doi:S0145212602000838 [pii]
15. Landriscina M, Laudiero G, Maddalena F, Amoroso MR, Piscazzi A, Cozzolino F, Monti M, Garbi C, Fersini A, Pucci P, Esposito F (2010) Mitochondrial chaperone Trap1 and the calcium binding protein Sorcin interact and protect cells against apoptosis induced by antiblastic agents. Cancer Res 70 (16):6577-6586. doi:10.1158/0008-5472.CAN-10-1256
0008-5472.CAN-10-1256 [pii]
16. Parekh HK, Deng HB, Choudhary K, Houser SR, Simpkins H (2002) Overexpression of sorcin, a calcium-binding protein, induces a low level of paclitaxel resistance in human ovarian and breast cancer cells. Biochem Pharmacol 63 (6):1149-1158. doi:S000629520200850X [pii]
17. Qu Y, Yang Y, Liu B, Xiao W (2010) Comparative proteomic profiling identified sorcin being associated with gemcitabine resistance in non-small cell lung cancer. Med Oncol 27 (4):1303-1308. doi:10.1007/s12032-009-9379-5
18. Zhou Y, Xu Y, Tan Y, Qi J, Xiao Y, Yang C, Zhu Z, Xiong D (2006) Sorcin, an important gene associated with multidrug-resistance in human leukemia cells. Leuk Res 30 (4):469-476. doi:S0145-2126(05)00331-0 [pii]
10.1016/j.leukres.2005.08.024
19. Yague E, Armesilla AL, Harrison G, Elliott J, Sardini A, Higgins CF, Raguz S (2003) P-glycoprotein (MDR1) expression in leukemic cells is regulated at two distinct steps, mRNA stabilization and translational initiation. J Biol Chem 278 (12):10344-10352. doi:10.1074/jbc.M211093200
M211093200 [pii]
20. Su Y, Cheng X, Tan Y, Hu Y, Zhou Y, Liu J, Xu Y, Xie Y, Wang C, Gao Y, Wang J, Cheng T, Yang C, Xiong D, Miao H (2012) Synthesis of a dual functional anti-MDR tumor agent PH II-7 with elucidations of anti-tumor effects and mechanisms. PLoS One 7 (3):e32782
21. Lombardo Y, Filipovic A, Molyneux G, Periyasamy M, Giamas G, Hu Y, Trivedi PS, Wang J, Yague E, Michel L, Coombes RC (2012) Nicastrin regulates breast cancer stem cell properties and tumor growth in vitro and in vivo. Proc Natl Acad Sci U S A 109 (41):16558-16563. doi:10.1073/pnas.1206268109
1206268109 [pii]
22. Bergers G, Hanahan D (2008) Modes of resistance to anti-angiogenic therapy. Nat Rev Cancer 8 (8):592-603
23. Charafe-Jauffret E, Ginestier C, Birnbaum D (2009) Breast cancer stem cells: tools and models to rely on. BMC Cancer 9:202. doi:10.1186/1471-2407-9-202
1471-2407-9-202 [pii]
24. Thiery JP, Acloque H, Huang RY, Nieto MA (2009) Epithelial-mesenchymal transitions in development and disease. Cell 139 (5):871-890. doi:10.1016/j.cell.2009.11.007
S0092-8674(09)01419-6 [pii]
25. Singh A, Settleman J (2010) EMT, cancer stem cells and drug resistance: an emerging axis of evil in the war on cancer. Oncogene 29 (34):4741-4751. doi:10.1038/onc.2010.215
onc2010215 [pii]

26. Gottesman MM, Fojo T, Bates SE (2002) Multidrug Resistance in Cancer: Role of ATP-dependent transporters. Nature Reviews Cancer 2:48-58
27. Kakarala M, Wicha MS (2007) Cancer stem cells: implications for cancer treatment and prevention. Cancer J 13 (5):271-275. doi:10.1097/PPO.0b013e318156da4e
00130404-200709000-00001 [pii]
28. Bastid J (2012) EMT in carcinoma progression and dissemination: facts, unanswered questions, and clinical considerations. Cancer Metastasis Rev 31 (1-2):277-283. doi:10.1007/s10555-011-9344-6
29. Ksiazkiewicz M, Markiewicz A, Zaczek AJ (2012) Epithelial-mesenchymal transition: a hallmark in metastasis formation linking circulating tumor cells and cancer stem cells. Pathobiology 79 (4):195-208. doi:10.1159/000337106
000337106 [pii]
30. Zheng BB, Zhang P, Jia WW, Yu LG, Guo XL (2012) Sorcin, a potential therapeutic target for reversing multidrug resistance in cancer. J Physiol Biochem 68 (2):281-287
31. Maddalena F, Laudiero G, Piscazzi A, Secondo A, Scorziello A, Lombardi V, Matassa DS, Fersini A, Neri V, Esposito F, Landriscina M (2011) Sorcin induces a drug-resistant phenotype in human colorectal cancer by modulating Ca(2+) homeostasis. Cancer Res 71 (24):7659-7669. doi:10.1158/0008-5472.CAN-11-2172
0008-5472.CAN-11-2172 [pii]
32. Qi J, Liu N, Zhou Y, Tan Y, Cheng Y, Yang C, Zhu Z, Xiong D (2006) Overexpression of sorcin in multidrug resistant human leukemia cells and its role in regulating cell apoptosis. Biochem Biophys Res Commun 349 (1):303-309. doi:S0006-291X(06)01840-7 [pii]
10.1016/j.bbrc.2006.08.042
33. Farrell EF, Antaramian A, Rueda A, Gomez AM, Valdivia HH (2003) Sorcin inhibits calcium release and modulates excitation-contraction coupling in the heart. J Biol Chem 278 (36):34660-34666. doi:10.1074/jbc.M305931200
M305931200 [pii]
34. Rizzuto R, Pozzan T (2006) Microdomains of intracellular Ca2+: molecular determinants and functional consequences. Physiol Rev 86 (1):369-408. doi:86/1/369 [pii]
10.1152/physrev.00004.2005
35. Chua HL, Bhat-Nakshatri P, Clare SE, Morimiya A, Badve S, Nakshatri H (2007) NF-kappaB represses E-cadherin expression and enhances epithelial to mesenchymal transition of mammary epithelial cells: potential involvement of ZEB-1 and ZEB-2. Oncogene 26 (5):711-724
36. Hoshino H, Miyoshi N, Nagai K, Tomimaru Y, Nagano H, Sekimoto M, Doki Y, Mori M, Ishii H (2009) Epithelial-mesenchymal transition with expression of SNAI1-induced chemoresistance in colorectal cancer. Biochem Biophys Res Commun 390 (3):1061-1065. doi:10.1016/j.bbrc.2009.10.117
S0006-291X(09)02108-1 [pii]
37. Rosano L, Cianfrocca R, Spinella F, Di Castro V, Nicotra MR, Lucidi A, Ferrandina G, Natali PG, Bagnato A (2011) Acquisition of chemoresistance and EMT phenotype is linked with activation of the endothelin A receptor pathway in ovarian carcinoma cells. Clin Cancer Res 17 (8):2350-2360. doi:10.1158/1078-0432.CCR-10-2325
1078-0432.CCR-10-2325 [pii]
38. Davis FM, Kenny PA, Soo ET, van Denderen BJ, Thompson EW, Cabot PJ, Parat MO, Roberts-Thomson SJ, Monteith GR (2011) Remodeling of purinergic receptor-mediated Ca2+ signaling as a consequence of EGF-induced epithelial-mesenchymal transition in breast cancer cells. PLoS One 6 (8):e23464

39. Hu J, Qin K, Zhang Y, Gong J, Li N, Lv D, Xiang R, Tan X (2011) Downregulation of transcription factor Oct4 induces an epithelial-to-mesenchymal transition via enhancement of Ca2+ influx in breast cancer cells. Biochem Biophys Res Commun 411 (4):786-791
40. Chen J, Wang M, Xi B, Xue J, He D, Zhang J, Zhao Y (2012) SPARC is a key regulator of proliferation, apoptosis and invasion in human ovarian cancer. PLoS One 7 (8):e42413. doi:10.1371/journal.pone.0042413
PONE-D-12-08336 [pii]
41. Rudland PS, Platt-Higgins A, Renshaw C, West CR, Winstanley JH, Robertson L, Barraclough R (2000) Prognostic significance of the metastasis-inducing protein S100A4 (p9Ka) in human breast cancer. Cancer Res 60 (6):1595-1603
42. Wang G, Platt-Higgins A, Carroll J, de Silva Rudland S, Winstanley J, Barraclough R, Rudland PS (2006) Induction of metastasis by S100P in a rat mammary model and its association with poor survival of breast cancer patients. Cancer Res 66 (2):1199-1207
43. Chen M, Bresnick AR, O'Connor KL (2012) Coupling S100A4 to Rhotekin alters Rho signaling output in breast cancer cells. Oncogene 2012 Sep 10. doi: 10.1038/onc.2012.383

44. Chen H, Yuan Y, Zhang C, Luo A, Ding F, Ma J, Yang S, Tian Y, Tong T, Zhan Q, Liu Z (2012) Involvement of S100A14 protein in cell invasion by affecting expression and function of matrix metalloproteinase (MMP)-2 via p53-dependent transcriptional regulation. J Biol Chem 287 (21):17109-17119
45. Lu D, Chen S, Tan X, Li N, Liu C, Li Z, Liu Z, Stupack DG, Reisfeld RA, Xiang R (2012) Fra-1 promotes breast cancer chemosensitivity by driving cancer stem cells from dormancy. Cancer Res 72 (14):3451-3456
46. Sajithlal GB, Rothermund K, Zhang F, Dabbs DJ, Latimer JJ, Grant SG, Prochownik EV (2010) Permanently blocked stem cells derived from breast cancer cell lines. Stem Cells 28 (6):1008-1018. doi:10.1002/stem.424
47. Ling H, Sylvestre JR, Jolicoeur P (2010) Notch1-induced mammary tumor development is cyclin D1-dependent and correlates with expansion of pre-malignant multipotent duct-limited progenitors. Oncogene 29 (32):4543-4554
48. Hanahan D, Weinberg RA (2011) Hallmarks of cancer: the next generation. Cell 144 (5):646-674. doi:10.1016/j.cell.2011.02.013
S0092-8674(11)00127-9 [pii]
49. Kowanetz M, Ferrara N (2006) Vascular endothelial growth factor signaling pathways: therapeutic perspective. Clin Cancer Res 12 (17):5018-5022
50. Patton AM, Kassis J, Doong H, Kohn EC (2003) Calcium as a molecular target in angiogenesis. Curr Pharm Des 9 (7):543-551
51. Lodola F, Laforenza U, Bonetti E, Lim D, Dragoni S, Bottino C, Ong HL, Guerra G, Ganini C, Massa M, Manzoni M, Ambudkar IS, Genazzani AA, Rosti V, Pedrazzoli P, Tanzi F, Moccia F, Porta C (2012) Store-operated Ca2+ entry is remodelled and controls in vitro angiogenesis in endothelial progenitor cells isolated from tumoral patients. PLoS One 7 (9):e42541
52. Scheel C, Weinberg RA (2012) Cancer stem cells and epithelial-mesenchymal transition: concepts and molecular links. Semin Cancer Biol 22 (5-6):396-403

Figure legends

Fig. 1 Sorcin silencing increases drug sensitivity. (**a**) Sorcin expression at mRNA (real-time PCR; *upper panel*) and protein (western blot, *left lower panel;* densitometry analysis using Image J, *right lower panel*) levels in MDA-MB-231 and MCF-7 cells. (**b**) Confirmation of sorcin knockdown in individual clones (MDA-E3 and MDA-D4; MDA-NC is a randomly selected negative control clone); Sorcin levels were determined by real-time RT-PCR and western blot analyses as in **a**. (**c**) Cell growth rate. Cells (1×10^4) were plated in each well of a 12-well plate and counted with a haematocytometer for up to 7 days. (**d**) MTT assays to determine the sensitivity of transfected MDA-MB-231 cells. Adriamycin (*left panel*) and etoposide (*right panel*). IC_{50} values were calculated from drug sensitivity curves from three independent experiments (Supplementary Fig. S1). (**e**) Apoptosis analysis by annexin V staining. Cells were treated with 10 µg/ml etoposide for 48 h and then stained with annexin V-FITC and propidium iodide. Apoptotic cells (annexin V-positive, propidium iodide-negative), were determined by flow cytometry. Numerical data represent mean ± SEM based on three independent experiments. *P<0.05; **P<0.01; ***P<0.001. Pictorial data shows a representative of three independent replicates

Fig. 2 Sorcin silencing inhibits EMT in MDA-MB-231 cells. (**a**) Bright field images of MDA-MB-231 cells showing a mesenchymal, spindle-like morphology (control clone) and a cobblestone-like epithelial shape in those expressing a sorcin targeting hairpin (MDA-E3 and MDA-D4 clones). (**b**) Wound healing ability of MDA-MB-231 cells transfected with sh targeting sorcin (MDA-E3 and MDA-D4) or vector control (MDA-NC). Confluent cell monolayers were wounded as described in Material and Methods and wound closure was monitored by microscopy after 24 h. (**c**) Transwell migration assay (*upper panels*) and Matrigel invasion assay (*lower panels*) of sorcin-depleted MDA-MB-231 cells. Cell were stained

with crystal violet (magnification: ×200). (**d**) Quantification of migration and invasion after counting the cells (See also Supplementary Fig. S2a). (**e**) E-cadherin and (**f**) ZEB-1 expression at mRNA (real-time PCR; (*histograms*) and (**g**) protein (western blot, *left panel;* Image J densitometry analysis, *right panel*) levels in sorcin-depleted MDA-MB-231 cells. (**h**) VEGF expression at mRNA (real-time PCR; *left panel*) and protein (ELISA*; right panel*) levels in sorcin-depleted MDA-MB-231 cells. Numerical data represent the mean ± SEM of three independent experiments. *P<0.05; **P<0.01; ***P<0.001. Pictorial data shows a representative of three independent replicates

Fig. 3 Suppression of sorcin reduces the stem cell sub-population of MDA-MB-231 cells. (**a**) Flow cytometry plots for CD44 and CD24 of MDA-MB-231 cells transfected with sh targeting sorcin (MDA-E3 and MDA-D4 clones) or vector control (MDA-NC clone). Gating was set to unstained cells. The percentage of cells in each quadrant is shown. Cells in Q1 ($CD44^{+}CD24^{-}$) are associated with a stem-like subpopulation. (**b**) Flow cytometry analysis of ALDH activity. Cells were assayed with ALDEFLUOR® assay kit in the presence (*upper panels*) and absence (*lower panels*) of the ALDH inhibitor DEAB. Percentage of cells with ALDH activity (gate) is shown. Gating in the control was set up to a maximum of 1% of cells. See also Supplementary Fig. S2b. (**c**) Mammorsphere formation in sorcin-depleted MDA-MB-231 cells. Pictures show a representative mammosphere from each “stem-like” cell taken at x100. Histogram shows the quantification of mammospheres in each well of a 6-well plate. See also Supplementary Fig. S2c. (**d**) Anchorage independent growth in soft agar of sorcin-depleted MDA-MB-231 cells. Picture shows a representative Petri dish after staining with MTT. Histogram data represents the average number of colonies counted in randomly-choosen 5 visual fields under the microscope (magnification x40). Numerical data represent mean ± SEM based on three

independent experiments. **P<0.01; ***P<0.001

Fig. 4 Silencing of sorcin inhibits MDA-MB-231 tumor formation and metastasis *in vivo.* (**a-c**) Nude mice (4 per group) were injected with either sorcin-depleted MDA-MB-231 (MDA-E3 and MDA-D4 clones) or control (MDA-NC clone) cells into the mammary fat pad. Tumor volume (**a**) and final tumor weight (**b**) were monitored up to 33 days, when tumors were removed from the primary site. Lung micrometastases were observed after H&E staining (**c**, arrow indicates areas of invasion; 40x magnification; bar represents 100 µm) and their frequency calculated (**c**, *lower panel*). (**d**) Sorcin and E-cadherin (*CDH-1*) mRNA expression determined by real-time PCR in primary tumors at 33 days post-injection. The brackets show the mean ± SEM. (**e**) VEGF expression (real-time PCR, left panel; ELISA, per ml of plasma normalized to primary tumor weight, right panel). *P<0.05; **P<0.01

Fig. 5 Sorcin regulates motility and invasion in several cancer cell lines**.** A549 and HT1080 cells were transiently transfected with siRNAs targeting sorcin (*siSorcin*) or a scrambled control (*siNC*). MCF-7 cells were stably transfected with a sorcin-overexpression lentivector (*Sorcin*) or an empty vector control (*EV*). (**a**) Sorcin mRNA expression determined by real-time PCR. Left panel, A549 cells; middle panel HT1080 cells; right panel, MCF-7 cells. (**b**) Transwell migration assay and Matrigel invasion assay in A549 and HT1080 cells and (**C**) MCF-7 cells . Pictures show crystal violet staining of cells in the transwells; magnification ×200. Histograms show quantification of the number of cells per field. Numerical data represent mean ± SEM of three independent experiments. *P<0.05; **P<0.01; ***P<0.001

Figure 1
Click here to download high resolution image

Figure 1 Hu et al

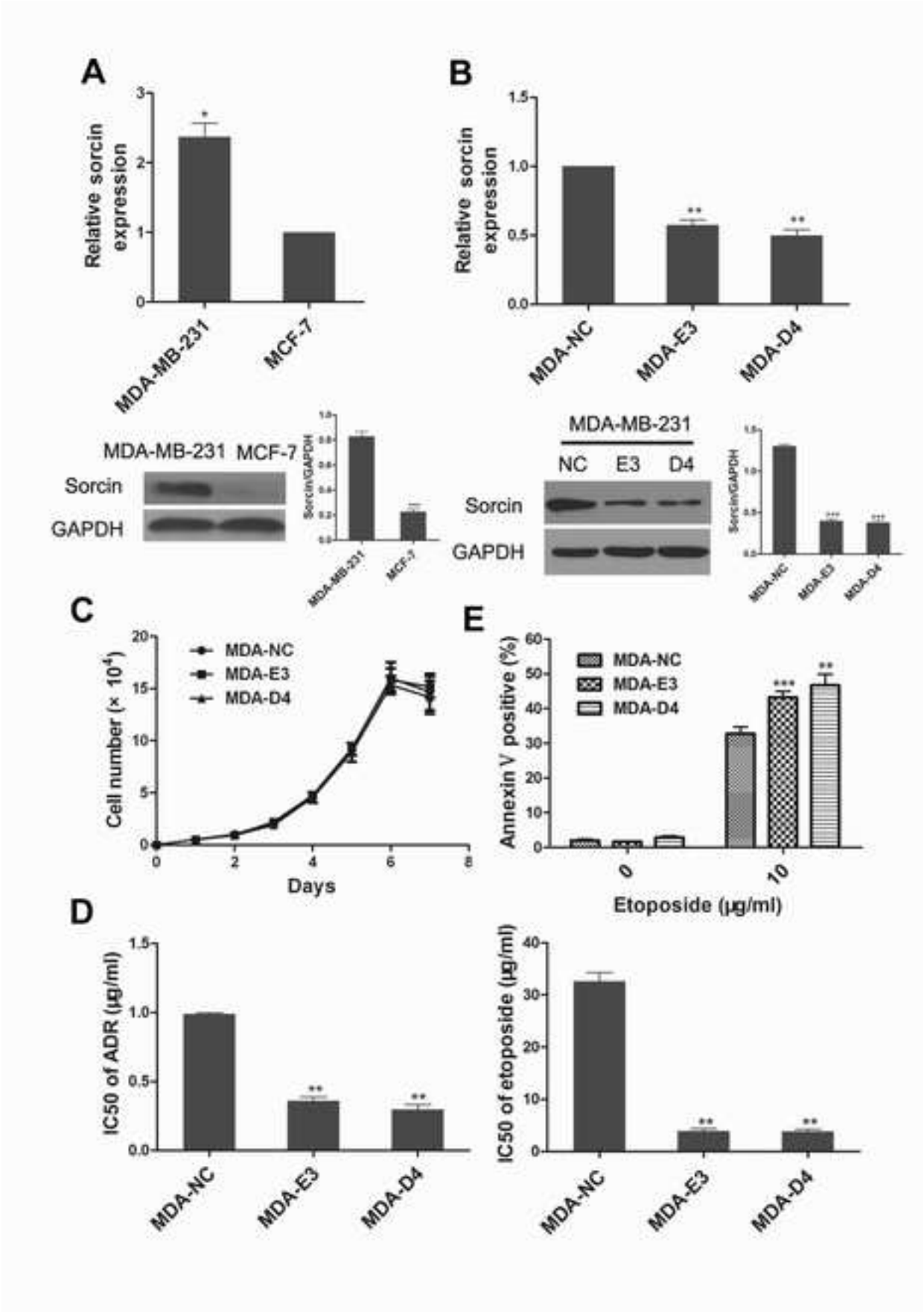


Figure 2
Click here to download high resolution image

Figure 2 Hu et al

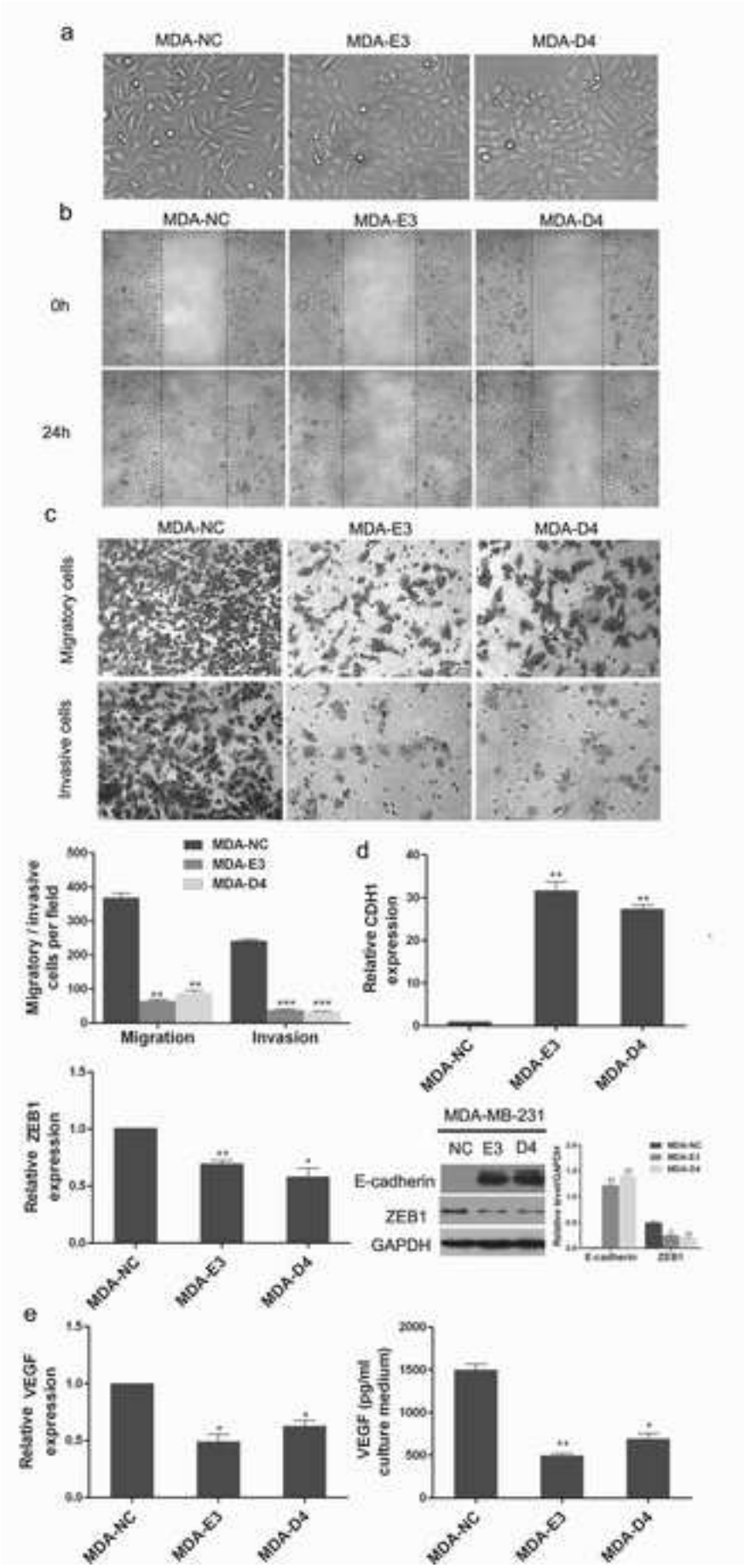


Figure 3
Click here to download high resolution image

Figure 3 Hu et al

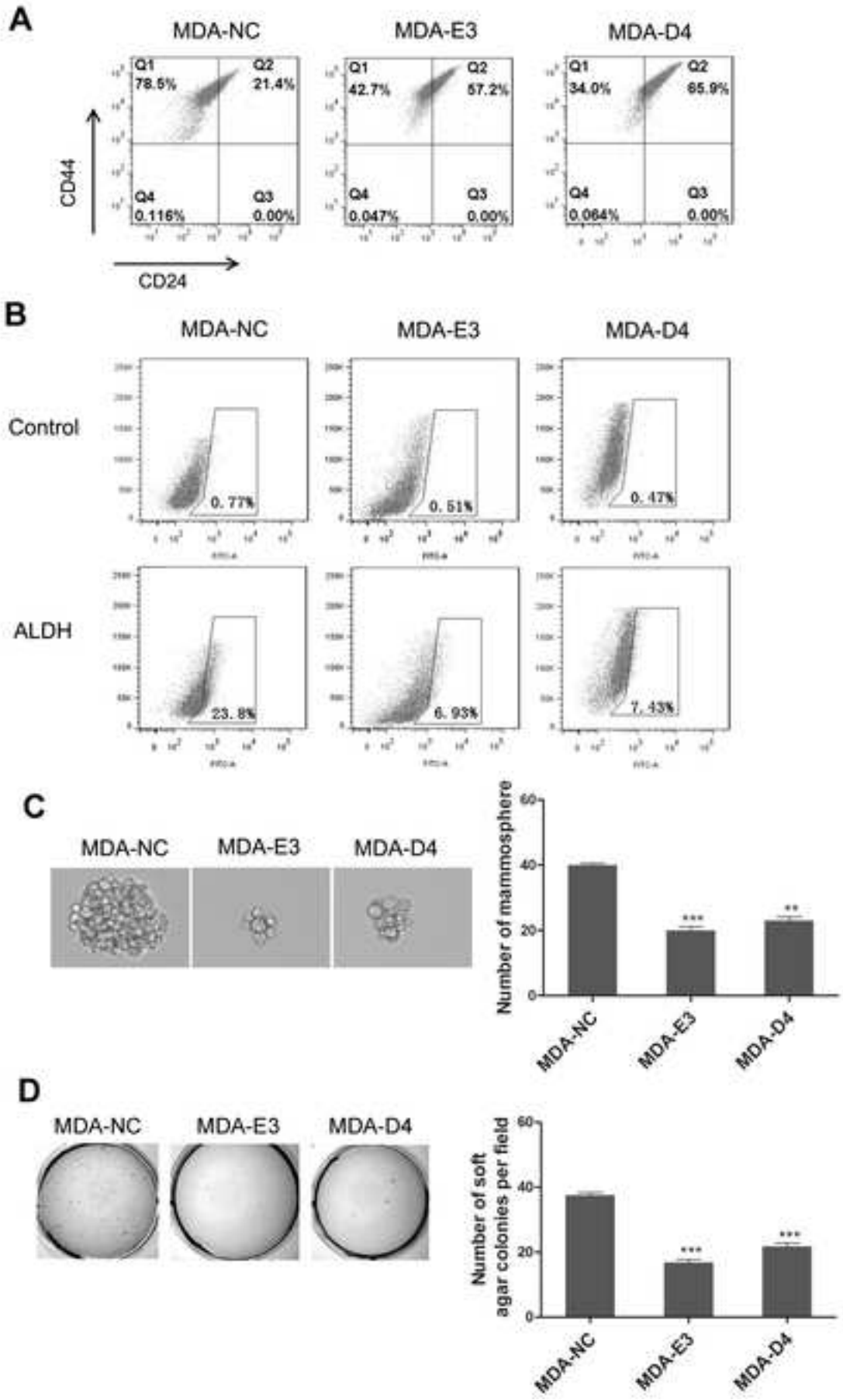
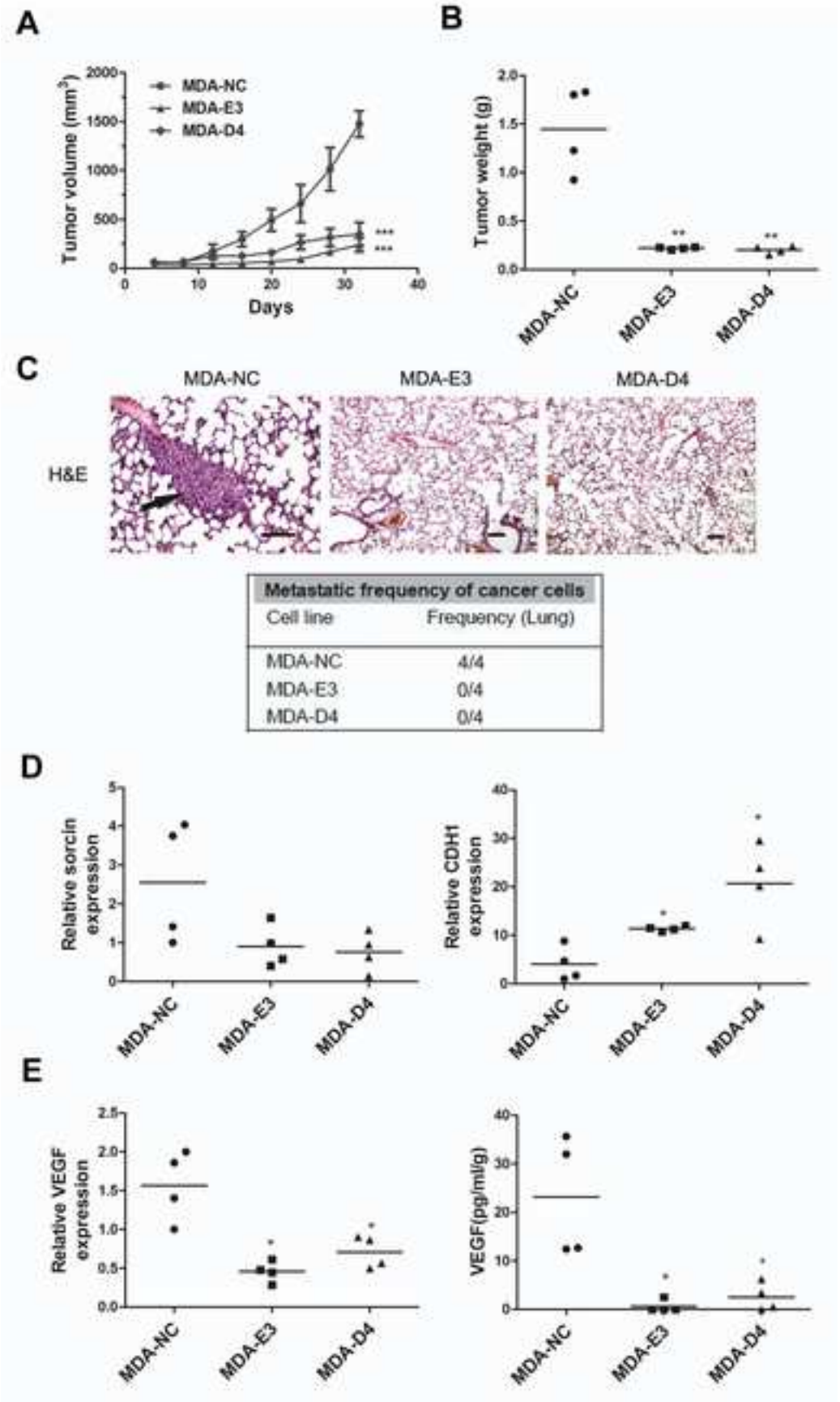


Figure 4
Click here to download high resolution image

Figure 4 Hu et al



Metastatic frequency of cancer cells	
Cell line	Frequency (Lung)
MDA-NC	4/4
MDA-E3	0/4
MDA-D4	0/4

Figure 5
Click here to download high resolution image

Figure 5 Hu et al

